

## Chemical Function Based Pharmacophore Generation of Endothelin-A Selective Receptor Antagonists

Oliver F. Funk,<sup>\*,†</sup> Viktor Kettmann,<sup>‡</sup> Jan Drimal,<sup>§</sup> and Thierry Langer<sup>\*,†</sup>

Department of Pharmaceutical Chemistry, Institute of Pharmacy, University of Innsbruck, Innrain 52a, A-6020 Innsbruck, Austria, Faculty of Pharmacy, Comenius University, Odbojarov 10, SK-83232, Bratislava, and Institute of Experimental Pharmacology, Slovak Academy of Sciences, Dubravská Cesta 9, SK-84216, Bratislava

Received September 22, 2003

Both quantitative and qualitative chemical function based pharmacophore models of endothelin-A (ET<sub>A</sub>) selective receptor antagonists were generated by using the two algorithms HypoGen and HipHop, respectively, which are implemented in the Catalyst molecular modeling software. The input for HypoGen is a training set of 18 ET<sub>A</sub> antagonists exhibiting IC<sub>50</sub> values ranging between 0.19 nM and 67 μM. The best output hypothesis consists of five features: two hydrophobic (HY), one ring aromatic (RA), one hydrogen bond acceptor (HBA), and one negative ionizable (NI) function. The highest scoring Hip Hop model consists of six features: three hydrophobic (HY), one ring aromatic (RA), one hydrogen bond acceptor (HBA), and one negative ionizable (NI). It is the result of an input of three highly active, selective, and structurally diverse ET<sub>A</sub> antagonists. The predictive power of the quantitative model could be approved by using a test set of 30 compounds, whose activity values spread over 6 orders of magnitude. The two pharmacophores were tested according to their ability to extract known endothelin antagonists from the 3D molecular structure database of Derwent's World Drug Index. Thereby the main part of selective ET<sub>A</sub> antagonistic entries was detected by the two hypotheses. Furthermore, the pharmacophores were used to screen the Maybridge database. Six compounds were chosen from the output hit lists for in vitro testing of their ability to displace endothelin-1 from its receptor. Two of these are new potential lead compounds because they are structurally novel and exhibit satisfactory activity in the binding assay.

### Introduction

The endothelins (ET) are 21 amino acid peptides that are mainly released by vascular endothelial cells.<sup>1</sup> There are three known subtypes, namely, ET-1, ET-2, and ET-3, binding to at least two types of G-protein-coupled receptors, ET<sub>A</sub> and ET<sub>B</sub>.<sup>2</sup>

Although ET<sub>A</sub> and ET<sub>B</sub> share great structural homology, these receptors have diverse affinity to the three types of endothelin. Whereas the ET<sub>A</sub> receptor has a higher affinity to ET-1 and ET-2 than to ET-3, the ET<sub>B</sub> receptor binds all three peptides equally strong.<sup>3</sup> Principally located on vascular smooth muscle cells,<sup>4</sup> the ET<sub>A</sub> receptor mediates vasoconstriction by activation of phospholipase C<sup>5</sup> and induces vascular smooth muscle cell proliferation.<sup>6</sup> The ET<sub>B</sub> receptor is abundantly expressed on vascular endothelial cells. Depending on its tissue location, it mediates vasorelaxation by release of nitric oxide and prostacyclin or vasoconstriction.<sup>7–10</sup> Furthermore, it participates in regulating the endogenous endothelin levels by inducing its elimination.<sup>11</sup>

ET-1 is the most potent endogenous vasoconstrictor known so far. Elevated levels of ET-1 and of cardiac ET<sub>A</sub> receptors and down-regulation of ET<sub>B</sub> receptors were

verified in disease states such as essential and pulmonary hypertension, congestive heart failure, and arteriosclerosis, which are associated with excessive vasoconstriction and smooth muscle cell proliferation.<sup>10,12–17</sup> Therefore, antagonism of the ET<sub>A</sub> receptors is expected to be an effective way for treating these diseases. A comprehensive overview on the diverse classes of ET antagonists is given in refs 18 and 19.

Oral administration of the unselective ET antagonist Bosentan to patients suffering from severe chronic heart failure resulted in an acute improvement of hemodynamic parameters.<sup>20</sup> However, as far as morbidity and mortality are concerned, no long-term benefits could be achieved.<sup>21</sup> Nevertheless, ET antagonists are of great benefit in treatment of pulmonary hypertension, which cannot be relieved with conventional therapies.<sup>22</sup> Furthermore, selective ET<sub>A</sub> blockers have shown more benefiting hemodynamic effects than their unselective analogues.<sup>23,24</sup> These findings could lead to new indications, e.g., chronic heart failure or hypertension.

To gain more insight into structure–activity relationships and to obtain access to new potential lead candidates by using in silico screening techniques, we generated chemical feature based pharmacophore models of ET<sub>A</sub> selective antagonists by using Accelry's Catalyst software.<sup>25</sup> The models were validated and finally used as queries for 3D database mining.

### General Methodology

For the generation of our chemical function based ET<sub>A</sub> models, we applied HypoGen<sup>26</sup> and HipHop,<sup>27,28</sup> the two

\* To whom correspondence should be addressed. For O.F.F.: phone, +43 512 5075268; fax, +43 512 507 5269; e-mail, oliver.funk@gmx.net. For T.L.: phone, +43 512 507 5252; fax, +43 512 507 5269; e-mail, thierry.langer@uibk.ac.at.

<sup>†</sup> University of Innsbruck.

<sup>‡</sup> Comenius University.

<sup>§</sup> Institute of Experimental Pharmacology, Slovak Academy of Sciences.

hypothesis generation algorithms implemented in the Catalyst software package. HypoGen tries to construct a pharmacophore that correlates best the three-dimensional arrangement of features in a given set of training compounds with the corresponding pharmacological activities. To ensure the statistic relevance of the calculated model, this training set should contain at least 16 compounds together with their activity values. These should originate from comparable binding assays and spread equally over at least 4 orders of magnitude. The resulting hypotheses are three-dimensional arrangements of several default feature types (e.g., hydrogen bond acceptor, hydrogen bond donor, hydrophobic, ring aromatic, positive ionizable) located at defined positions (location constraints). These are surrounded by certain spatial tolerance spheres, assessing the area in space that should be assigned by the corresponding chemical functions of the matched molecule. Each of the features occupies a certain weight that is proportional to its relative contribution to biological activity. Hydrogen bond acceptors, donors, and aromatic rings additionally include a vector, defining the direction of the interaction.

The HypoGen algorithm tries to find hypotheses that are common among the active compounds of the training set but do not reflect the inactive ones. It observes the principle of Ockham's razor, "plurality should not be posited without necessity",<sup>29</sup> thus constructing a model that correlates best with measured activities and that consists of as few features as possible.

During a HypoGen run, three phases are passed through: (a) Pharmacophores that are common among the most active compounds are elaborated in the constructive phase. (b) Those pharmacophores that fit the inactive training set members are abolished in the subtractive phase. (c) The remaining hypotheses are refined in the optimization phase. Thereby random translations of features, rotations of vectored features, and the removal or addition of features from the models are performed. Each perturbation is evaluated by consideration of three cost components, the Error, the Configuration, and the Weight Cost, which will be pointed out later. The 10 hypotheses with the lowest cost are printed to the output file. HypoGen pharmacophores can estimate the activity values of compounds by regressing their geometric fit value versus  $-\log(\text{activity})$ .

If there is not enough suitable biological data available to accomplish the considerably high demands of a HypoGen training set, one can apply the HipHop process. This algorithm calculates hypotheses by aligning those features that are common to the molecules of a given training set. It must contain the conformational models of preferably diverse and highly active compounds; exact activity values are not needed for model generation. The feature-based 3D pharmacophoric alignments are computed in a three-step procedure: (a) Each generated conformer is examined for the presence of chemical features. (b) Three-dimensional configurations of chemical features, common to the input molecules, are determined. (c) The hypotheses are ranked on the basis of the portion of training set members that fit the proposed pharmacophore and the frequency of its occurrence. The better the hypothesis fits the training set

compounds and the more frequently it occurs, the higher is the probability that it is not a result of a random correlation.

Both HypoGen and HipHop deliver plausible models of a pharmacophore, conclusively termed as hypothesis in Catalyst. These do not render coercively the true pharmacophore but can only correlate the information given by the training set. Thus, the quality of the output strongly depends on how comprehensively the reality is reflected by the input data. There are several techniques to verify the reliability of the calculated hypotheses, e.g., estimation of test compounds activities, retrieval of active candidates from 3D molecular structure databases, or analysis of the hypotheses cost parameters printed to the output file. Many successful applications confirm that Catalyst is a useful tool for the discovery of new leads, acting on specific pharmacological targets.<sup>30-39</sup>

**Important Output Parameters.** The HypoGen process provides a multiple hypothesis output for proving the reliability of the outcome data. An essential evaluation criterion is the hypothesis cost analysis that is applied by HypoGen to rank the generated pharmacophores. As default, the 10 lowest cost hypotheses are written to the output file.

A Weight, an Error, and a Configuration Cost value are summed up to the Total Cost value. These three components could be described as follows: Each feature of a hypothesis represents certain orders of magnitude of the compounds' activity. With the default setting of 0.302, the represented orders of magnitude are kept as close to 2 as possible. The weight component is a value that increases in a Gaussian form as these function weights in a model deviate from the ideal value of 2. Increase of the root-mean-square (rms) divergence between estimated and measured activities for the training set molecules leads to a higher Error Cost value. The Configuration Cost is a Fixed Cost that quantifies the entropy of the hypothesis space. That means that if the input information is too multiplex (e.g., training set molecules are too flexible and/or have too many features), this would lead to an effusive number of hypotheses as outcome of the subtractive phase of the hypothesis generation process. In the standard HypoGen mode, the configuration cost should not exceed a maximum value of 17 (corresponds to a number of  $2^{17}$  pharmacophore models). Higher values would lead more likely to a chance correlation of the generated hypothesis, since Catalyst cannot consider more than  $2^{17}$  models in the optimization phase and so the rest is left out of the process. The HypoGen module performs two additional theoretical cost calculations (represented in bit units) to help the user in assessing the statistical significance of the generated hypothesis. The Fixed Cost is the lowest possible cost representing a hypothetical, simplest model that fits all data perfectly. It is calculated by adding the minimum achievable Error and Weight Cost and the constant Configuration Cost. The Null Cost represents the maximum cost of a pharmacophore with no features and estimates activity to be the average of the training set molecules' activity data. Its absolute value is equal to the maximum occurring Error Cost. The greater the difference between these two cost values and the closer the cost

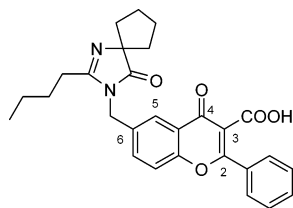


**Figure 1.** AT-antagonistic lead structure (**A**) modified in the SAR studies reported by Ishizuka et al.<sup>42</sup>

of the generated hypothesis (Total Cost) is to the Fixed Cost, the more statistically significant the hypothesis is supposed to be. According to randomized studies, a cost difference of 40–60 bits between the Total Cost and the Null Cost indicates a 75–90% chance of representing a true correlation in the data.<sup>26</sup>

## Results and Discussion

**1. HypoGen Model.** Recently Ishizuka et al. reported a novel class of ET<sub>A</sub> receptor antagonists that were derived from an angiotensin (AT) receptor antagonist.<sup>42</sup> Compound **A** shown in Figure 1 was the starting AT-antagonistic structure to be modified. The inhibitory activities had been tested by displacement of [<sup>125</sup>I]ET-1 from the rat ET<sub>A</sub> receptor expressed in rat aorta smooth muscle cells. The compounds of this test series are well suited for an application to Catalyst because of their rather rigid structures. This enhances the probability of obtaining a pharmacophore that matches closely the actual spatial arrangement of the particular functions, though the structure of the receptor is not known. The structure–activity relationship (SAR) study revealed that the most important substituents on the 2H-chromene skeleton are the *m,p*-methylenedioxyphenyl, the carboxyl, the hydrophobic residue, and the isopropoxy group at positions 2, 3, 4, and 6. In relation to the *m,p*-methylenedioxy moiety, there is very little tolerance. All performed structural variations induced a loss in activity. These underlying interactions cannot be explained solely by distinct chemical functions. Rather, there are additional spatial effects that increase the ligands' activity by 2 orders of magnitude. Probably at this part of the receptor site, there is a binding pocket that is exactly filled in with the *m,p*-methylenedioxy group and that contains a hydrogen bond donor interacting with the electron lone pair of the perfectly positioned para oxygen atom. Since HypoGen cannot deal with these kinds of spatial problems yet, the program has to carry out a simplification of the actual binding relations in generating pharmacophore models. At the position within the binding site corresponding to substituents at position 6, there seems to be a binding pocket that interacts very specifically with the isopropoxy group, since the slightest variation reduced the compounds' ability to displace ET<sub>A</sub>. However, according to former SAR studies,<sup>43–45</sup> in this region of the receptor there seem to be multiple hydrophobic areas to bind diverging hydrophobic substituents. The carboxyl group may be exchanged by any negative ionizable function without great loss of activity. There has to be an ion–ion interaction, since only compounds bearing functions that are charged negatively at physiologic pH values show high affinity to the receptor. At the 4-position, various linear, branched, and cyclic aliphatic or substi-

tuted and unsubstituted aromatic groups with an optimum length of 6–9 Å are crucial for ET<sub>A</sub> receptor affinity. They may vary in a wide range as far as steric extent and spatial arrangement are concerned. Best activities are achieved by a *p*-anisyl residue (e.g., compound **1**), but also an *n*-butyl group (e.g., compound **2**) is accepted with only a minimal loss in activity. The wide tolerance of spatial extent and arrangement of substituents at position 4 indicates a considerable flexible hydrophobic binding pocket in the corresponding receptor site.

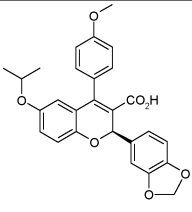
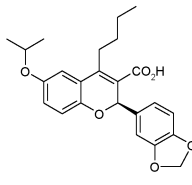
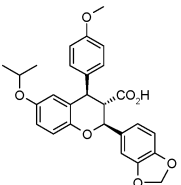
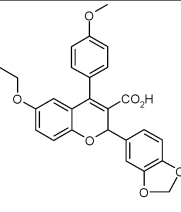
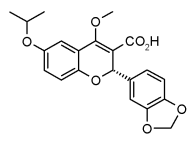
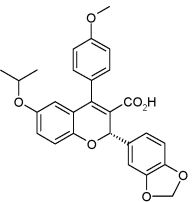
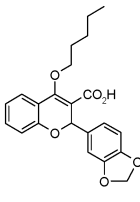
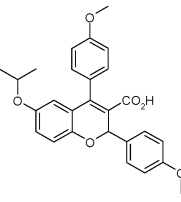
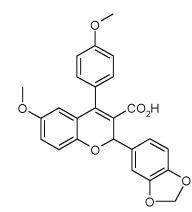
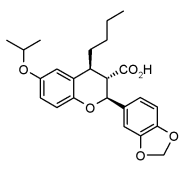
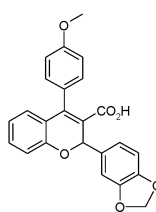
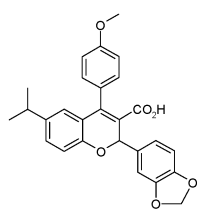
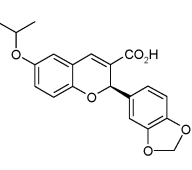
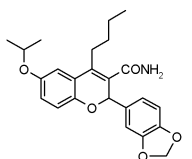
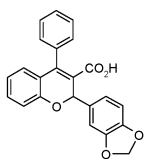
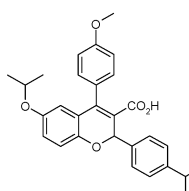
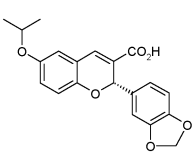
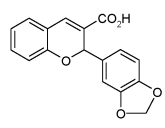
We chose 18 of the tested structures as the training set for a HypoGen run. Their molecular structures and ET<sub>A</sub> antagonistic activity values are listed in Table 1. For editing of the molecules, the Catalyst 2D/3D sketcher was used. Since molecules can adjust their conformations in order to bind to a receptor site, conformational models were generated to ensure a maximum coverage in feature space. Therefore, the “best quality” conformational search option was applied. The energy threshold, kept during the calculation, was set to 20 kcal/mol above the global energy minimum. Catalysts conformational search is based on CHARMM force field parameters<sup>46</sup> and a Poling technique<sup>47</sup> that promotes conformational variation within the accessible space by penalizing a newly generated conformer if it is too similar to any other conformer in the set. For the selection of the training set compounds, we took into account that there was no redundancy in the input information concerning both structural features and activity ranges. Hence, the chance of obtaining a pharmacophore model with high statistical relevance in predicting biological activity of ET<sub>A</sub> antagonists was increased. The selected compound activity is spread equally over a range of 6 orders of magnitude (i.e., 0.19–67 000 nm).

The training-set was applied to a run with the HypoGen algorithm. The “catHypo.forceAbsoluteStereochemistry” parameter was set to 1 to force the automatic hypothesis routines to consider only the supplied configurations and no enantio- or diastereomers.

The uncertainty of the compounds' activity input was adopted from the Catalyst 4.7 manual. The herein recommended value of 3 represents the ratio range of uncertainty in the measured activity values due to statistical straggling. For the construction of hypotheses, a set of default chemical feature templates exist. The sulfonamide function (pks ≈ 7–8) is an important part of several ET<sub>A</sub> antagonists, but it does not satisfy the negative ionizable function provided within Catalyst by default. Thus, we added this feature by applying the Exclude/Or Quick Tool in order to make the program recognize all kinds of acidic sulfonamides as acidic functions.

As mentioned before, four chemical feature types such as hydrogen bond acceptor, hydrophobic, ring aromatic, and negative ionizable are of crucial relevance for the displacement of ET from its receptor. Hence, these feature types were used in the HypoGen run. The spacing parameter was set to 5. This enables HypoGen to consider features of the training set molecules with a minimum distance of 5 pm (default value: 297 pm) as two distinct functions. Hence, for example, the two oxygen atoms of a carboxyl group may be recognized as

**Table 1.** Chemical Structures<sup>a</sup> of the 18 Training Set Molecules<sup>b</sup> Applied to HypoGen Pharmacophore Generation (ET<sub>A</sub> Activities Are Given as IC<sub>50</sub> Values)

			
<b>1</b> (IC <sub>50</sub> : 0.19nM)	<b>2</b> (IC <sub>50</sub> : 0.42nM)	<b>3</b> (IC <sub>50</sub> : 1.3nM)	<b>4</b> (IC <sub>50</sub> : 3.8nM)
			
<b>5</b> (IC <sub>50</sub> : 5.2nM)	<b>6</b> (IC <sub>50</sub> : 15nM)	<b>7</b> (IC <sub>50</sub> : 29nM)	<b>8</b> (IC <sub>50</sub> : 35nM)
			
<b>9</b> (IC <sub>50</sub> : 74nM)	<b>10</b> (IC <sub>50</sub> : 77nM)	<b>11</b> (IC <sub>50</sub> : 86nM)	<b>12</b> (IC <sub>50</sub> : 110nM)
			
<b>13</b> (IC <sub>50</sub> : 240nM)	<b>14</b> (IC <sub>50</sub> : 410nM)	<b>15</b> (IC <sub>50</sub> : 780nM)	<b>16</b> (IC <sub>50</sub> : 1200nM)
			
<b>17</b> (IC <sub>50</sub> : 1600nM)	<b>18</b> (IC <sub>50</sub> : 6700nM)		

<sup>a</sup> All 2D chemical structures were edited with ISIS/Draw 2.1 software (MDL Information Systems, ISIS/Draw 2.1, 1990–1996). <sup>b</sup> Ishizuka et al.<sup>42</sup>

two hydrogen bond acceptors. All other parameters were kept as default. Among the outcome 10 lowest cost hypotheses, only hypothesis 3 has two hydrophobic, one hydrogen bond acceptor, one ring aromatic, and one negative ionizable feature in a spatial arrangement that was expected because of preceding SAR analysis. The HypoGen algorithm does not set a feature onto the central 2H-chromene skeleton, since this moiety is also present in the inactive molecules. The pharmacophore consists only of those features that contribute mainly to the increase of activity. Thus, such a model is able to detect preferably diverse structures in a database mining experiment. Figure 2 shows the mapping of one of the most active training set compounds **3** on the best hypothesis of the second HypoGen run, obtained by

using the best fit compare option on the Generate Hypothesis Workbench. The model shows a good correlation between the measured and the estimated activity values of the training set (0.953) but high rms (0.856) and bad Configuration Cost values (18.77). Since the maximum Configuration Cost of 17 was exceeded, it has to be considered that not all hypotheses were regarded in the optimization phase. To achieve further improvement, a second HypoGen run was carried out with constraints on the numbers of the regarded functions as follows: hydrophobic, min 2, max 2; hydrogen bond acceptor, min 1, max 1; ring aromatic, min 1, max 1; negative ionizable, min 1, max 1. All other parameters were kept as pointed out before. Thereby the correlation, rms, and Configuration Cost values of the initial hy-

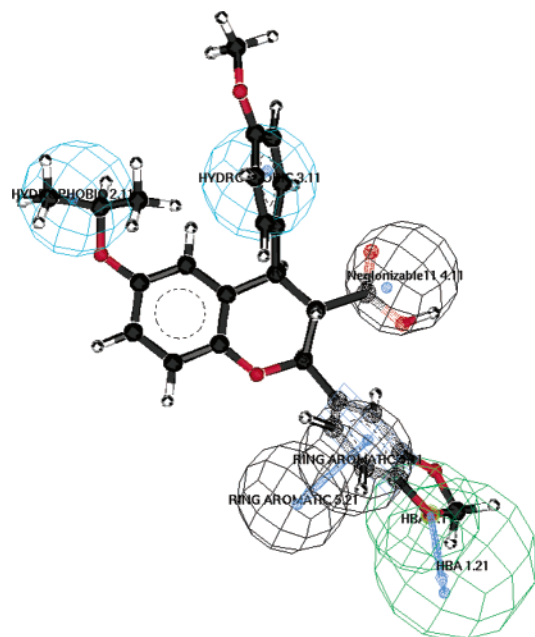


**Figure 2.** Mapping of the highly active training set compound **3** on the best HypoGen model.

hypothesis were found to be improved by the resulting best pharmacophore from 0.953 to 0.981, from 0.856 to 0.574, and from 18.77 to 14.97, respectively.

**2. Evaluation of the HypoGen Model. 2.1. Cost Analysis.** The total Fixed Cost of the run is 76.6, and the cost of the Null Hypothesis is 131.13. The cost ranges between the best hypothesis (Total Cost: 81.69), the Null Hypothesis, and the Fixed Cost amount to 49.44 and 5.05. As mentioned before, because of the fact that the best hypothesis' Total Cost is much closer to the Fixed Cost than to the Null Cost, the high correlation coefficient of 0.981 and the low rms value of 0.574 indicate a reliable ability of the generated pharmacophore model to predict training set compounds activities and confirm that it did not come about by chance.

**2.2. Score Hypothesis.** The training set was submitted to a score hypothesis process. Within this procedure

**Table 2.** Output of the Score Hypothesis Process

compd	measured activity <sup>a</sup> (nM)	estimated activity (nM)	error factor <sup>b</sup>	energy of mapping conformer (kcal/mol)
1	0.19	0.47	2.47	10.2
2	0.42	0.44	1.05	14.2
3	1.3	1.4	1.08	15.1
4	3.8	8.5	2.24	14.2
5	5.2	2.4	-2.17	7.3
6	15	7.8	-1.92	12.3
7	29	22	-1.32	11.5
8	35	5	-7.00	13.8
9	74	79	1.07	15.3
10	77	80	1.04	7.3
11	86	98	1.14	4.7
12	110	56	-1.96	12.1
13	240	310	1.29	5.6
14	410	740	1.80	9.8
15	780	720	-1.08	1.4
16	1200	64	-18.75	3.3
17	1600	820	-1.95	8.2
18	67000	230000	-3.43	1.7

<sup>a</sup> Ishizuka et al.<sup>42</sup> <sup>b</sup> The error factor is computed as the ratio of the measured activity to the activity estimated by the hypothesis or the inverse if Estimated is greater than Measured.

the activity of every single training set member is estimated by the hypothesis. The result exhibited a correlation of 96% between measured and predicted activities. The hypothesis can discriminate closely between stereoisomers (compounds **1**, **6** and **13**, **17**) and saturated and unsaturated chromene skeletons (compounds **1**, **2** and **3**, **10**). Only one compound (**16**) was predicted with an error higher than 1 order of magnitude and another (**8**) with an error factor of  $-7$  (see Table 2). Both compounds contain a *p*-methoxy but no *m,p*-methylenedioxy substructure. The oxygen atom of the *p*-methoxy group maps the hydrogen bond acceptor feature, but the hypothesis cannot detect that there is no *m,p*-methylenedioxy moiety that increases the affinity to the receptor by 2 orders of magnitude due to the optimum steric fit (see Figure 3). As we stated before, HypoGen is not able to deal with these kinds of spatial problems yet. When these two outliers are left out of the score hypothesis spreadsheet, the correlation could be improved to 98.3%. A visual analysis of the training set compounds mappings onto the hypothesis was

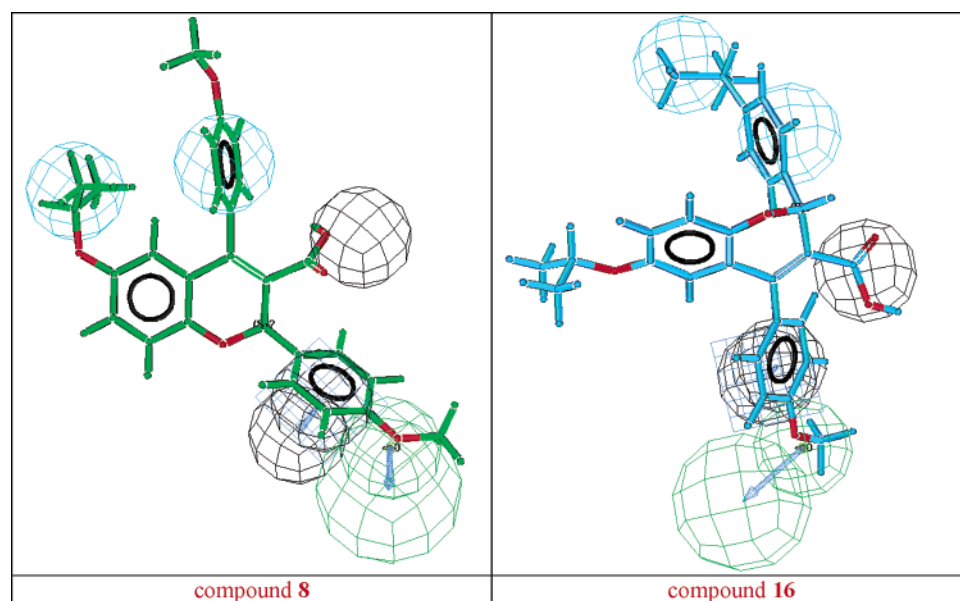


**Figure 3.** Mapping of compounds **8** and **16** resulting from the score hypothesis process.

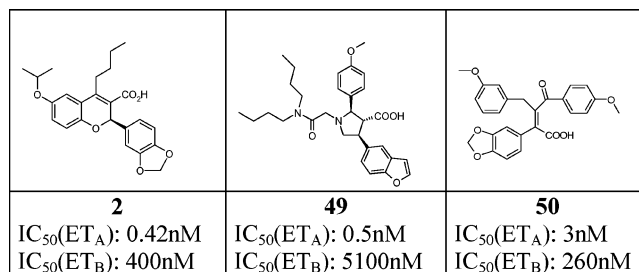
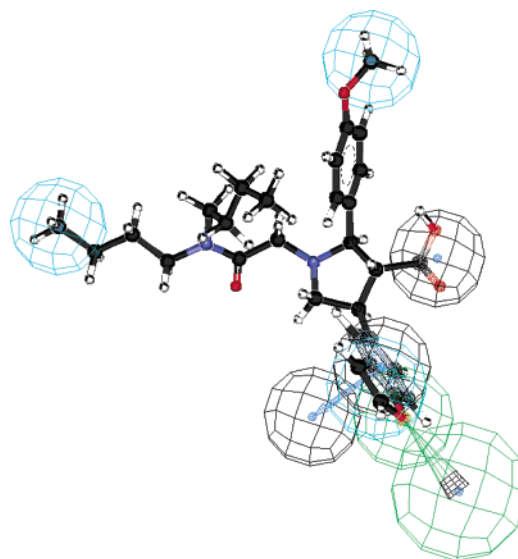
**Table 3.** Output Parameters of the 10 Lowest Cost Hypotheses Resulting from the Statistical Evaluation Procedure According to the Fischer Method<sup>48</sup>

hypothesis	correlation	rms	total cost
1	0.86	1.45	97.93
2	0.89	1.33	98.85
3	0.80	1.70	101.51
4	0.81	1.64	103.06
5	0.84	1.58	103.66
6	0.79	1.72	103.68
7	0.82	1.62	103.69
8	0.83	1.61	104.13
9	0.82	1.64	105.10
10	0.81	1.67	106.334
best hypothesis	0.98	0.57	81.69

carried out to verify if the good correlation did not arise by random overlay. All structures, except compound **16**, fit the pharmacophore in the expected, reasonable way in conformity with preceding SAR analysis (e.g., see Figure 2). This result confirms that our hypothesis is a reliable model for describing the SAR in the training set.

**2.3. Fisher Test.** To further evaluate the statistical relevance of the model, the Fischer method<sup>48</sup> was applied. With the aid of the CatScramble program, the experimental activities in the training set were scrambled randomly, and the resulting training set was used for a HypoGen run. Thereby all parameters were adopted from the initial HypoGen calculation. This procedure was reiterated 49 times. None of the outcome hypotheses had a lower cost score than the initial hypothesis. According to the software documentation and the literature available, this result indicates that there is a 98% chance for hypothesis 1 to represent a true correlation in the training set activity data.<sup>30,64</sup> Table 3 lists the 10 lowest Total Cost values of the resulting 49 hypotheses.

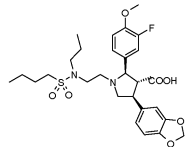
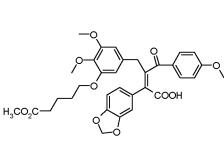
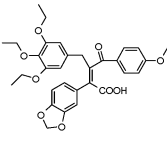
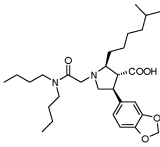
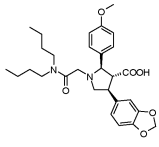
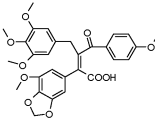
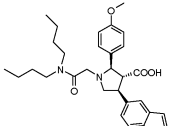
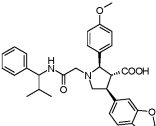
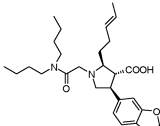
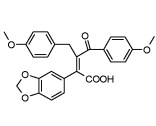
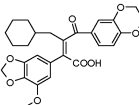
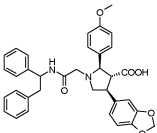
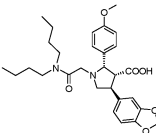
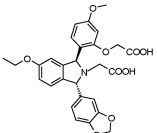
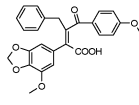
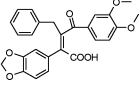
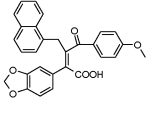
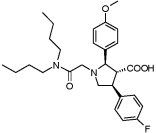
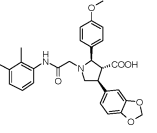
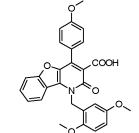
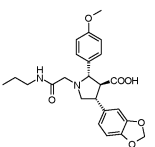
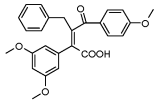
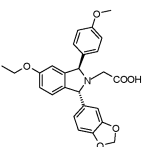
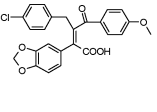
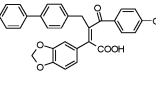
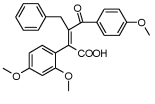
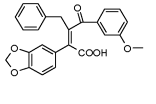
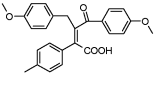
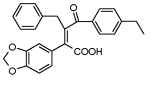
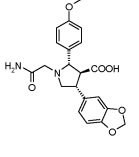
**2.4. Test Set.** The main purpose of a quantitative model is to identify active structures and to forecast their actual activity accurately. To verify if the hypothesis can also predict the activity of compounds that are structurally distinct from those included in the training set, we applied a test set of 30 compounds<sup>44,45,50–52,54–56,65,66</sup> (see Table 4). The activity values spread over a range of 6 orders of magnitude. The molecules and the corresponding conformational models were edited in the same way as pointed out before. For the estimation we used the BestEst option of the ViewHypothesis Workbench. Out of the 30 measured activity values, 21 were predicted with an error factor less than 10. The 9 remaining estimations were carried out with an error factor below 100. On average, the error factor amounts to 12.6 (Table 5). Since all test set members are from different structural classes as the training set compounds and since their activity values were determined with different assay systems by different research groups, a more precise estimation was not expected. Agreeable to preceding molecular modeling studies,<sup>30,31</sup> the error factor of 10 up to 100 is sufficient to roughly classify the compounds according to their activities. Summarizing, it could be demonstrated that the hypothesis is able to graduate ET<sub>A</sub> antagonists of different structural classes, not included in the training set, by their affinity to the receptor.

**Figure 4.** Chemical structures of the three ET<sub>A</sub>-selective training set molecules applied to HipHop pharmacophore generation.**Figure 5.** Mapping of training set compound **49** on the best HipHop model.

**2.5. HipHop Model.** Besides HypoGen, we also applied the HipHop algorithm to generate a qualitative common features model. Therefore, we chose three highly active and ET<sub>A</sub> selective training compounds from different structural classes, **2**,<sup>42</sup> **49**,<sup>56</sup> and **50**,<sup>52</sup> displayed in Figure 4). The “catHypo.forceAbsoluteStereochemistry” was set to 1 as mentioned before. To force HipHop to render only those pharmacophores that do not miss any feature of the training set members, the “Principal” value was set to 2 and the “Maximum Omitted Features” value was set to 0 for all three structures. Additionally, the Misses, Feature Misses, and Complete Misses parameter were set to 0. (For a detailed description of these input parameters, see the Catalyst 4.7 Tutorial: [http://www.accelrys.com/doc/life/catalyst47/tutorials/Catalyst47\\_2002TOC.html](http://www.accelrys.com/doc/life/catalyst47/tutorials/Catalyst47_2002TOC.html).) The number of considered chemical functions was restricted to two or three hydrophobics, one ring aromatic, one negative ionizable, and one hydrogen bond acceptor. The best hypothesis of the outcome consists of three hydrophobic, one negative ionizable, one hydrogen bond acceptor, and one ring aromatic feature. Figure 5 shows the mapping of the most selective training set compound **49** on the HipHop pharmacophore.

**3. Database Search.** Either of the two best hypotheses was used as a query in a screening of three-dimensional multiconformational molecular structure databases. The Derwent's World Drug Index database (WDI)<sup>57</sup> was searched using the “Fast Flexible Search Databases/Spreadsheets” option. This algorithm uses

**Table 4.** Chemical Structures<sup>m</sup> of the 30 ET<sub>A</sub>-antagonists Used as Test Set for Validation of the Predictive Power of the HypoGen Pharmacophore

				
<b>19<sup>a</sup></b>	<b>20<sup>b</sup></b>	<b>21<sup>c</sup></b>	<b>22<sup>d</sup></b>	<b>23<sup>e</sup></b>
				
<b>24<sup>c</sup></b>	<b>25<sup>f</sup></b>	<b>26<sup>g</sup></b>	<b>27<sup>d</sup></b>	<b>28<sup>c</sup></b>
				
<b>29<sup>h</sup></b>	<b>30<sup>g</sup></b>	<b>31<sup>e</sup></b>	<b>32<sup>i</sup></b>	<b>33<sup>c</sup></b>
				
<b>34<sup>c</sup></b>	<b>35<sup>c</sup></b>	<b>36<sup>f</sup></b>	<b>37<sup>k</sup></b>	<b>38<sup>l</sup></b>
				
<b>39<sup>e</sup></b>	<b>40<sup>c</sup></b>	<b>41<sup>i</sup></b>	<b>42<sup>c</sup></b>	<b>43<sup>c</sup></b>
				
<b>44<sup>c</sup></b>	<b>45<sup>c</sup></b>	<b>46<sup>c</sup></b>	<b>47<sup>c</sup></b>	<b>48<sup>e</sup></b>

<sup>a</sup> Jae et al.<sup>43</sup> <sup>b</sup> Patt et al.<sup>65</sup> <sup>c</sup> Patt et al.<sup>52</sup> <sup>d</sup> Liu et al.<sup>66</sup> <sup>e</sup> Winn et al.<sup>45</sup> <sup>f</sup> Tasker et al.<sup>56</sup> <sup>g</sup> Liu et al.<sup>44</sup> <sup>h</sup> Doherty et al.<sup>50</sup> <sup>i</sup> Kukkola et al.<sup>55</sup> <sup>k</sup> von Geldern et al.<sup>49</sup> <sup>l</sup> Mederski et al.<sup>54</sup> <sup>m</sup> All 2D chemical structures were edited with ISIS/Draw2.1 software (MDL Information Systems, ISIS/Draw2.1, 1990–1996).

only the precomputed conformations for fitting the hypothesis during a search. The optional, more time-consuming “Best Flexible Search Databases/Spreadsheets” process can thereby vary the existing conformers up to an energy threshold of 9.5 kcal/mol. Concerning both procedures, only those structures that map all features of the pharmacophore template are retrieved. To exclude those compounds that are unlikely to be

GPCR ligands because of their high molecular weight,<sup>58,59</sup> the hit lists were pruned by a 700 g/mol molecular weight cutoff. Out of the 48 500 entries deposited in the WDI, the quantitative model detected 143 structures altogether (0.3% of the whole WDI). Among these, there were 12 highly active endothelin antagonists from different structural classes. Four of these possess a strong and selective affinity to the ET<sub>A</sub> receptor. The

**Table 5.** Activity Values Predicted by the HypoGen Hypothesis, Experimental Data of the Test Set Compounds, and Corresponding Error Factors

compd	measured activity IC <sub>50</sub> <sup>a</sup> (nM)	estimated activity IC <sub>50</sub> (nM)	error factor <sup>b</sup>
19	0.04	0.075	1.7
20	0.05	0.028	1.8
21	0.12	0.02	6.0
22	0.29	0.21	1.4
23	0.31	0.08	3.9
24	0.5	0.021	23.8
25	0.5	0.19	2.6
26	0.7	0.26	2.7
27	0.78	0.35	2.2
28	1.8	8.9	4.9
29	3.5	1.9	2.1
30	3.9	0.48	8.1
31	4.62	0.63	7.3
32	5.4	14	2.6
33	6.7	19	2.8
34	11	4.9	2.2
35	14	0.4	35
36	14	25	1.8
37	16	0.25	64
38	21	5.1	4.1
39	45.3	0.55	82.4
40	46	3.8	12.1
41	96	200	2.1
42	110	36	3.1
43	200	26	7.7
44	300	4900	16.3
45	500	16	31.3
46	570	25	22.8
47	630	4300	6.8
48	2030	23000	11.3
	mean value of error factor: <sup>b</sup>		12.6

<sup>a</sup> Shizuka et al.<sup>42</sup> <sup>b</sup> The error factor is computed as the ratio of the measured activity to the activity estimated by the hypothesis or the inverse if Estimated is greater than Measured.

more selective common features model retrieved 12 structures (0.03% of the whole WDI). Five of these are unselective, and three are selective ET<sub>A</sub> antagonists with high efficacy. By investigation of the WDI meta-data and the Ensemble database,<sup>60</sup> 60 entries of ET antagonists could be found in the WDI database altogether. Thirty-six of these are supposed to have a binding mode distinct from that of the training set compounds, since their structures are entirely different. As a matter of principle, Catalyst hypotheses can only detect those compounds that have in common the same binding site at the receptor and accordingly coincidental binding features. Eight candidates of the remaining 24 entries could be stated as ET<sub>A</sub> selective. Five of these could be detected by our hypotheses (see Figure 6). There are several circumstances that may prevent the mapping of active structures. In our case, one of the ET<sub>A</sub> selective candidates could not be detected because it is enlisted as its lacton prodrug. Conclusively, it could not fit the negative ionizable feature of the hypothesis. Another two leave a hydrophobic sphere because they do not possess the corresponding residue. Except for these three misses, all of the highly active ET<sub>A</sub> antagonists, which are supposed to have a similar binding mode, could be retrieved. This result is a significant confirmation for the calculated models' reliability.

The aim of our study was to detect new ET<sub>A</sub> antagonistic lead structures. Therefore, we screened the Maybridge database,<sup>61</sup> containing about 55 000 commercially available compounds, with our pharmacophore models. To obtain as many hits as possible, the "Best Flexible

PD-155080 <b>51</b> (preclinical) <sup>a</sup>	PD-156707 <b>52</b> (phase I) <sup>a</sup>	A-127722 <b>53</b> (preclinical) <sup>a</sup>
L-744453 <b>54</b> (preclinical) <sup>a</sup>	PD-151242 <sup>b</sup> <b>55</b>	

**Figure 6.** Structures and highest testing phases of the selective ET<sub>A</sub> antagonists detected in the WDI query. Footnote designations are defined as follows: (a) information about highest phase of testing from the Ensemble database (Prous Science Ensemble: A new database affording a unique, integrated view of drug information, <http://www.prous.com> (accessed 2000)); (b) no data about highest phase of testing available from the Ensemble database (Prous Science Ensemble: A new database affording a unique, integrated view of drug information, <http://www.prous.com> (accessed 2000)).

BTB 15187 <b>56</b> IC <sub>50</sub> (ET <sub>A</sub> ): 220nM	HTS 00155 <b>57</b> IC <sub>50</sub> (ET <sub>A</sub> ): 6.200nM	HTS00117 <b>58</b> 77% inh. at 10 <sup>-4</sup> M	S 08597 <b>59</b> 60% inh. at 10 <sup>-4</sup> M

**Figure 7.** Structures and experimental activity data of the extracted Maybridge compounds that exhibited in vitro activity.

Search Databases/Spreadsheets" option was applied. The query resulted in 498 hits with the HypoGen and in 5 hits with the HipHop hypothesis. In consideration of their high fit values and their availability, six identified structures were selected for in vitro testing of their ET<sub>A</sub> antagonistic activity. Two of the test candidates demonstrated moderate activity, and another two were able to displace [<sup>125</sup>I]ET-1 from its binding site at higher concentrations. Their structures and the mappings onto the corresponding hypothesis are displayed in Figures 7 and 8, respectively. The competitive binding curves for the four active compounds are shown in Figure 9. The measured IC<sub>50</sub> values for the two most potent structures are given in Table 6. The



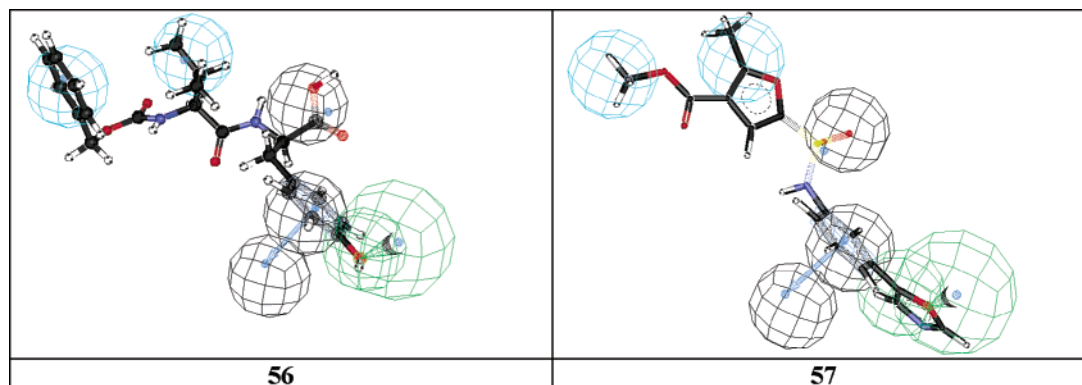


**Figure 8.** Mapping of compounds **56** and **57** on the best HypoGen model.

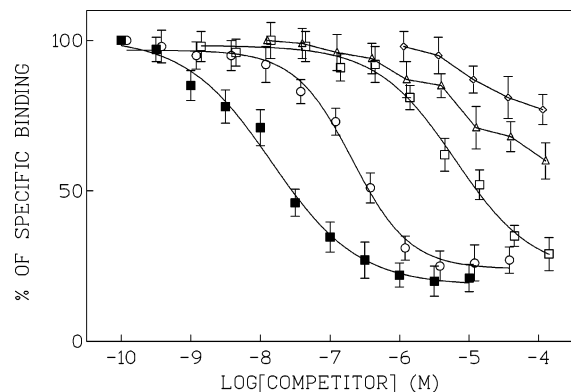


**Figure 9.** Inhibition of specific [ $^{125}\text{I}$ ]ET-1 (50 pM) binding to Vero cells by BTB 15187 (**56**) (open circles), HTS 00155 (**57**) (open squares), HTS 00117 (**58**) (open diamonds), S 08597 (**59**) (open triangles), and the standard compound BQ-123 (filled squares). Each point represents the mean of three independent experiments, and bars are standard deviations of the mean.

**Table 6.** Affinity ( $\text{IC}_{50}$  Values) and Hill Coefficients ( $n_H$ ) of the Two Most Potent Competitors for [ $^{125}\text{I}$ ]ET-1 Binding Sites in Vero Cells<sup>a</sup>

compd	$\text{IC}_{50}$ (nM)	$n_H$
BTB 15187	$220 \pm 53$	$-1.00 \pm 0.03$
HTS 00155	$6.200 \pm 1.600$	$-0.91 \pm 0.04$
BQ-123 <sup>b</sup>	$25 \pm 7$	$-1.05 \pm 0.03$

<sup>a</sup> The values represent the mean  $\pm$  standard error of three separate measurements. <sup>b</sup> Standard compound, used for comparative purposes.

$\text{IC}_{50}$  values could not be determined for **59** and **58** because at the highest concentration tested ( $10^{-4}$  M), they were able to inhibit the specific [ $^{125}\text{I}$ ]ET-1 binding to only 60% and 77%, respectively (see Figure 9). The remaining two samples (HTS 01535 and HTS 04170) were totally unable to displace the [ $^{125}\text{I}$ ]ET-1 radioligand over the whole concentration range. The reason for this might be (1) total inactivity of these compounds or (2) their inactivity at concentrations lower than ca.  $10^{-7}$  M and aqueous insolubility at concentrations of ca.  $10^{-6}$  M and higher.

For the three compounds given in Table 6, the Hill coefficients were not significantly different from unity, indicating interaction with the single ( $\text{ET}_A$ ) binding site. The reliability of the results is documented by the  $\text{IC}_{50}$  of BQ-123 (25 nM; Table 6) which compares well with the value of 40 nM reported for this standard.<sup>62</sup>

Remarkably, the most active test candidate, **56**, had the highest fit value of all hits detected by the HipHop pharmacophore. Also, the HypoGen model ranks this

compound as one of the top entries. There is an outstanding analogy between **56** and the highly selective  $\text{ET}_A$  antagonist **55**. Compound **57** contains an oxazole substructure instead of the 3,4-methylenedioxy group that is a common motif within many  $\text{ET}_A$  antagonists. Thus, **57** represents a promising candidate for further structural variations, which may result in highly active compounds without the 3,4-methylenedioxy moiety. Because of their properties, **56** and **57** are well suited candidates to be investigated as novel lead compounds acting on the endothelin system.

## Experimental Section

**Molecular Modeling Studies.** The molecular modeling calculations were accomplished on a SGI Octane double processor workstation running the Catalyst 4.7 package and Irix 6.5. The database mining, using the generated pharmacophore as a three-dimensional query, was executed on a Linux PC cluster.

**Biological Testing.** Human  $\text{ET}_A$  receptor binding affinity was determined using a standard procedure as described previously.<sup>40</sup> Briefly, green monkey renal tubular (Vero) cells were grown at 37 °C as monolayer cultures in minimal essential medium supplemented with 10% (v/v) fetal bovine serum, nonessential amino acids, and 100 U/mL each of penicillin and streptomycin in an atmosphere of 5%  $\text{CO}_2/95\%$  air. The whole-cell binding assays were performed in triplicate with the cells ( $2 \times 10^5$  cells/well) under polarized conditions (buffer I, in mmol/L: NaCl 135,  $\text{MgCl}_2$  1.0,  $\text{KH}_2\text{PO}_4$  0.44,  $\text{NaH}_2\text{PO}_4$  0.34,  $\text{NaHCO}_3$  2.6, HEPES 20.0, glucose 5.6, pH 7.4) in the presence of 50 pM [ $^{125}\text{I}$ ]ET-1 and either 500 nM ET-1 (to define nonspecific binding) or the test compound. After incubation (1 h) the bound radioligand was separated from the free one by a rapid filtration through the GF/C Whatman filters and washed with cold assay buffer. The radioactivity of the filters was measured by using a Packard Tri-Carb-300 CD scintillation counter (Packard Instruments, Downers Grove, IL). The binding data were expressed as a percentage of specific [ $^{125}\text{I}$ ]ET-1 binding (total binding in the presence of unlabeled ET-1) and analyzed by the curve-fitting software GraphPad InPlot.<sup>41</sup>

Stock solutions of the test compounds were prepared at a concentration of ca. 1 mM by dissolving 5 mg of the compound in 1 mL of DMSO and completed to 10 mL by addition of deoxygenated water. The concentrations in the range of ca.  $10^{-10}$ – $10^{-4}$  M were used in the binding assays, and the  $\text{ET}_A$ -selective antagonist BQ-123 was included as a standard to verify the sensitivity of the experiments. It was observed that while the solution of compounds BTB 15187 (**56**), HTS 00155 (**57**), HTS 00117 (**58**), and S 08597 (**59**) remained clear and pellucid over the whole concentration range, in the solution of HTS 01535 and HTS 04170 a precipitate appeared at concentrations  $10^{-6}$  M and higher, indicating very low solubility of the last two compounds in water. The relative binding affinity of the test compounds (and BQ-123) for the  $\text{ET}_A$

receptor in the Vero cells was measured by their ability to compete with the specific binding of [<sup>125</sup>I]ET-1.

## Conclusion

In our study we built a quantitative and a qualitative pharmacophore model applying two different ligand-based pharmacophore generation approaches, HypoGen and HipHop. The resulting best hypotheses consisted of five and six features, respectively. The pharmacophores' reliability in quantitative terms was verified in several validation procedures. Although the HypoGen training set was based on one single class of structurally related compounds, it is capable estimating the activity values of 30 compounds originating from other series accurately enough to assign them to different activity classes. The bigger part of selective ET<sub>A</sub> antagonists was extracted from the large 3D molecular structure database of Derwent's WDI. Remarkably, the HipHop derived model based on only three different ET<sub>A</sub> antagonists was 10 times more selective in the 3D database mining experiments than the quantitative approach (hit rate of 0.03% vs 0.3%). The two hypotheses were used as 3D queries in a mining of the Maybridge database. Six of the retrieved Maybridge compounds were selected for testing of their affinity to the ET<sub>A</sub> receptor. Two of these proved to be active at the ET<sub>A</sub> receptor. In summary, it could be demonstrated that pharmacophore models created with Catalyst are effective tools for the identification of new lead structures. Another 3D-QSAR analysis (i.e., based on CoMFA<sup>63</sup> or related methods) using the HypoGen training set would be an interesting additional approach to investigate important ligand-receptor interactions. However, the aim of the present study was to detect new lead compounds. Thus, we did not apply these methods because the resulting models in their present data format cannot be used for the mining of 3D databases.

In consideration of the enormous effort of in vitro screening of large compound libraries, the in silico database mining method presented in our study is a powerful and fast approach that could decisively reduce the cost of hit finding within the drug discovery and development process.

**Acknowledgment.** The authors thank Mag. K. Poptodorov, Mag. Dr. E. M. Krovat, Mag. T. Steindl, and Dr. G. Wolber for their steady advice and helpful collaborations. Dr. Rémy D. Hoffmann (Accelrys SARL, Paris) is thanked for performing the 3D database search in the Derwent World Drug Index.

## References

- Inoue, A.; Yanagisawa, M.; Kimura, S.; Kasuya, Y.; Miyachi, T.; et al. The Human Endothelin Family: Three Structurally and Pharmacologically Distinct Isopeptides Predicted by Three Separate Genes. *Proc. Natl. Acad. Sci. U.S.A.* **1989**, *86*, 2863–2867.
- Sakurai, T. Y.; Yanagisawa, M.; Masaki, T. Molecular Characterization of Endothelin Receptors. *Trends Pharmacol. Sci.* **1992**, *13*, 103–108.
- Saeki, T.; Ihara, M.; Fukuroda, T.; Yamagiwa, M.; Yano, M. [Ala<sup>1,3,11,15</sup>]endothelin-1 Analogs with ET-B Agonistic Activity. *Biochem. Biophys. Res. Commun.* **1991**, *179*, 286–292.
- Arai, H.; Hori, S.; Aramori, I.; Ohkubo, H.; Nakanishi, S. Cloning and Expression of a cDNA Encoding an Endothelin Receptor. *Nature* **1990**, *348*, 730–732.
- Panek, R. L.; Major, T. C.; Hingorani, G. P.; Dunbar, J. B.; Doherty, A. M.; et al. Importance of Secondary Structure for Endothelin Binding and Functional Activity. *Biochem. Biophys. Res. Commun.* **1992**, *183*, 572–576.
- Ohlstein, E. H.; Arleth, A.; Bruyan, H.; Elliott, J. D.; Sung, C. P. The Selective Endothelin ETA Receptor Antagonist BQ123 Antagonizes Endothelin-1-Mediated Mitogenesis. *Eur. J. Pharmacol.* **1992**, *225*, 347–350.
- Takayanagi, R.; Kitazumi, R.; Takasaki, C.; Ohnaka, K.; Aimoto, S.; et al. Presence of Non-Selective Type of Endothelin Receptor on Vascular Endothelium and Its Linkage to Vasodilation. *FEBS Lett.* **1991**, *282*, 103–106.
- Warner, T.; Mitchell, J.; De Nucci, G.; Vane, J. Endothelin-1 and Endothelin-3 Release EDRF from Isolated Perfused Arterial Vessels of the Rat and Rabbit. *J. Cardiovasc. Pharmacol.* **1989**, *13*, 85–88.
- De Nucci, G.; Thomas, R.; D'Orleans-Juste, P.; Antunes, E.; Walder, C.; et al. Pressor Effects of Circulating Endothelin Are Limited by the Release of Prostacyclin and Endothelium-Derived Relaxing Factor. *Proc. Natl. Acad. Sci. U.S.A.* **1988**, *85*, 9797–9800.
- Kiowski, W.; Sütsch, G.; Hunziker, P.; Muller, P.; Kim, J.; et al. Evidence for Endothelin-1-Mediated Vasoconstriction in Severe Chronic Heart Failure. *Lancet* **1995**, *346*, 732–736.
- Ishikawa, K.; Ihara, M.; Noguchi, K.; Mase, T.; Mino, N.; et al. Biochemical and Pharmacological Profile of a Potent and Selective Endothelin B-Receptor Antagonist, BQ-788. *Proc. Natl. Acad. Sci. U.S.A.* **1994**, *91*, 4892–4896.
- Stewart, D. J.; Levy, R. D.; Cernacek, P.; Langleben, D. C. Increased Plasma Endothelin-1 in Pulmonary Hypertension: Marker or Mediator of Disease? *Ann. Intern. Med.* **1991**, *114*, 464–469.
- Krum, H.; Viskoper, R. J.; Lacourciere, Y.; Budde, M.; Charlon, V. The Effect of an Endothelin-Receptor Antagonist, Bosentan, on Blood Pressure in Patients with Essential Hypertension. *N. Engl. J. Med.* **1998**, *338*, 784–790.
- Cardillo, C.; Kilcoyne, C. M.; Waclawiw, M.; Cannon, R. O.; Panza, J. A. Role of Endothelin in the Increased Vascular Tone of Patients with Essential Hypertension. *Hypertension* **1999**, *33*, 753–758.
- Moreland, S.; McMullen, D.; Delaney, C.; Lee, V.; Hunt, J. Venous Smooth Muscle Contains Vasoconstrictor ETB-like Receptors. *Biochem. Biophys. Res. Commun.* **1992**, *184*, 100–106.
- Stewart, D. Update on Endothelin. *Can. J. Cardiol.* **1998**, Suppl. D, 11D–13D.
- Zolk, O.; Quatteck, M. S.; Sitzler, G.; Schrader, T.; Nickenig, T.; et al. Expression of Endothelin-1, Endothelin-Converting-Enzyme and Endothelin Receptors in Chronic Heart failure. *Circulation* **1999**, *99*, 2118–2123.
- Wu, C. Recent Discovery and Development of Endothelin Receptor Antagonists. *Expert Opin. Ther. Pat.* **2000**, *10*, 1653–1668.
- Elliott, J. D.; Xiang, J. Endothelin Receptor Antagonists. In *Endothelin and Its Inhibitors*; Springer: Berlin, 2001; Chapter 9.
- Sütsch, G.; Kiowski, W.; Yan, X. W. Short-Term Oral Endothelin-Receptor Antagonist Therapy in Conventionally Treated Patients with Symptomatic Severe Chronic Heart Failure. *Circulation* **1998**, *98*, 2262–2268.
- Kalra, P. R.; Moon, J. C.; Coats, A. J. Do Results of the ENABLE (Endothelin Antagonist Bosentan for Lowering Cardiac Events in Heart Failure) Study Spell the End for Non-Selective Endothelin Antagonism in Heart Failure? *Int. J. Cardiol.* **2002**, *85*, 195–197.
- Maloney, J. P. Advances in the treatment of secondary pulmonary hypertension. *Curr. Opin. Pulm. Med.* **2003**, *9*, 139–143.
- Verhaar, M. C.; Strachan, F. E.; Newby, D. E.; Cruden, N. L.; Koomans, H. A.; et al. Endothelin-A Receptor Antagonist Mediated Vasodilatation is Attenuated by Inhibition of Nitric Oxide Synthesis and by Endothelin-B Receptor Blockade. *Circulation* **1998**, *97*, 752–756.
- Ohnishi, M.; Wada, A.; Tsutamoto, T.; Fukui, D.; Kinoshita, M. Comparison of the Acute Effects of a Selective Endothelin ET-A and a Mixed ET-A/ET-B Receptor Antagonist in Heart Failure. *Cardiovasc. Res.* **1998**, *39*, 617–624.
- Catalyst, version 4.7; Accelrys Inc., 9685 Scranton Road, San Diego, CA 92121.
- Li, H.; Sutter, J.; Hoffmann, R. HypoGen: An Automated System for Generating 3D Predictive Pharmacophore Models. In *Pharmacophore Perception, Development and Use in Drug Design*; International University Line: La Jolla, CA, 2000.
- Omohile, O.; Trope Mehl, C.; Trope Mehl, A. HipHop: Pharmacophores Based on Multiple Common-Feature Alignments. In *Pharmacophore Perception, Development and Use in Drug Design*; International University Line: La Jolla, CA, 2000.
- Barnum, D.; Greene, J.; Smellie, A.; Sprague, P. Identification of Common Functional Configurations among Molecules. *J. Chem. Inf. Comput. Sci.* **1996**, *36*, 563–571.
- English philosopher and Franciscan monk William of Ockham, 1285–1349.

- (30) Krovat, E. M.; Langer, T. Non-Peptide Angiotensin II Receptor Antagonists: Chemical Feature Based Pharmacophore Identification. *J. Med. Chem.* **2003**, *46*, 716–726.
- (31) Debnath, A. K. Pharmacophore Mapping of a Series of 2,4-Diamino-5-deazapteridine Inhibitors of Mycobacterium Avium Complex Dihydrofolate Reductase. *J. Med. Chem.* **2002**, *45*, 41–53.
- (32) Karki, R. G.; Kulkarni, M. V. A Feature Based Pharmacophore for Candida Albicans MyristoylCoA: Protein N-Myristoyltransferase Inhibitors. *Eur. J. Med. Chem.* **2001**, *36*, 147–163.
- (33) Kaminski, J. J.; Rane, D. F.; Snow, M. E.; Weber, L.; Rothofsky, M. L.; et al. Identification of Novel Farnesyl Protein Transferase Inhibitors Using Three-Dimensional Database Searching Methods. *J. Med. Chem.* **1997**, *40*, 4103–4112.
- (34) Hirashima, A.; Pan, C.; Kuwano, E.; Taniguchi, E.; Eto, M. Three-Dimensional Pharmacophore Hypotheses for the Locust Neuronal Octopamine Receptor (OAR3). Part 2: Agonists. *Bioorg. Med. Chem.* **1999**, *7*, 1437–1443.
- (35) Langer, T.; Hoffmann, R. D.; Daxenbichler, G.; Bachmair, F.; Begle, S. Chemical Function Based Pharmacophore Models as Suitable Filters for Virtual 3D-Database Screening. *J. Mol. Struct.: THEOCHEM* **2000**, *503*, 59–72.
- (36) Lopez-Rodriguez, M.; Porras, E.; Benhamu, B.; Ramos, J. A.; Morcillo, M. J.; et al. First Pharmacophoric Hypothesis for 5-HT7 Antagonism. *Bioorg. Med. Chem. Lett.* **2000**, *10*, 1097–1100.
- (37) Singh, J.; van Vlijmen, J.; Liao, Y.; Lee, W.; Cornebise, M.; et al. Identification of Potent and Novel  $\alpha_4\beta_1$  Antagonists Using in Silico Screening. *J. Med. Chem.* **2002**, *45*, 2988–2993.
- (38) Palomer, A.; Cabre, F.; Pascual, J.; Campos, J.; Trujillo, M. A.; et al. Identification of Novel Cyclooxygenase-2 Selective Inhibitors Using Pharmacophore Models. *J. Med. Chem.* **2002**, *45*, 1402–1411.
- (39) Kurogi, Y.; Miyata, K.; Okamura, T.; Hashimoto, K.; Tsutsumi, K.; et al. Discovery of Novel Mesangial Cell Proliferation Inhibitors Using a Three-Dimensional Database Searching Method. *J. Med. Chem.* **2001**, *44*, 2304–2307.
- (40) Drimal, J.; Bauerova, K.; Kettmann, V.; Knezl, V. C. Counteractive Adrenergic and Endothelin ETB-Receptor Subtype Signaling Modulate Proliferation in Monkey Renal Cells. *Biology* **2000**, *55*, 299–304.
- (41) Saavedra, J. *InPlot. A Nonlinear Least-Squares Curve-Fitting Program*, version 4.03; GraphPad Software Inc.: New York, 1992.
- (42) Ishizuka, N.; Matsumara, K.; Sakai, K.; Fujimoto, M.; Mihara, S.; et al. Structure–Activity Relationships of a Novel Class of Endothelin-A Receptor Antagonists and Discovery of Potent and Selective Receptor Antagonist, 2-(Benzo[1,3]dioxol-5-yl)-6-isopropoxy-4-(4-methoxyphenyl)-2H-chromene-3-carboxylic Acid (S-1255). 1. Study on Structure–Activity Relationships and Basic Structure Crucial for ETA Antagonism. *J. Med. Chem.* **2002**, *45*, 2041–2055.
- (43) Jae, H.; Winn, M.; Dixon, D. B.; Marsh, K. C.; Nguyen, B.; et al. Pyrrolidine-3-carboxylic Acids as Endothelin Antagonists. 2. Sulfonamide-Based ETA/ETB Mixed Antagonists. *J. Med. Chem.* **1997**, *40*, 3217–3227.
- (44) Liu, G.; Kozmina, N. S.; Winn, M.; von Geldern, T. W.; Chiou, W. J.; et al. Design, Synthesis, and Activity of a Series of Pyrrolidine-3-carboxylic Acid-Based, Highly Specific, Orally Active ETB Antagonists Containing a Diphenylmethylamine Acetamide Side Chain. *J. Med. Chem.* **1999**, *42*, 3679–3689.
- (45) Winn, M.; von Geldern, T. W.; Oppenorth, T. J.; Jae, H.; Tasker, A. S.; et al. 2,4-Diarylpyrrolidine-3-carboxylic Acids—Potent ETA Selective Endothelin Receptor Antagonists. 1. Discovery of A-127722. *J. Med. Chem.* **1996**, *39*, 1039–1048.
- (46) Brooks, B. R.; Brucolleri, R. E.; Olafson, B. D.; States, D. J.; Swaminathan, S.; et al. CHARMM: A Program for Macromolecular Energy Minimization, and Dynamic Calculations. *J. Comput. Chem.* **1983**, *4*, 187–217.
- (47) Smellie, A.; Teig, S. L.; Towbin, P. Poling: Promoting Conformational Coverage. *J. Comput. Chem.* **1995**, *16*, 171–187.
- (48) Fischer, R. The Principle of Experimentation, Illustrated by a Psycho-Physical Experiment. *The Design of Experiments*, 8th ed.; Hafner Publishing Co.: New York, 1966; Chapter II.
- (49) von Geldern, T. W.; Tasker, A. S.; Sorensen, B. K.; Winn, M.; Szczepankiewicz, B. G.; et al. Pyrrolidine-3-carboxylic Acids as Endothelin Antagonists. 4. Side Chain Conformational Restriction Leads to ET-B Selectivity. *J. Med. Chem.* **1999**, *42*, 3668–3678.
- (50) Elliott, J. D.; Lago, M. A.; Cousins, R. D.; Gao, A.; Leber, J. D.; et al. 1,3-Diarylindan-2-carboxylic Acids, Potent and Selective Non-Peptide Endothelin Receptor Antagonists. *J. Med. Chem.* **1994**, *37*, 1553–1557.
- (51) Doherty, A. M.; Patt, W. C.; Edmunds, J. J.; Berryman, K. A.; Reisdorph, B. R.; et al. Discovery of a Novel Series of Orally Active Non-Peptide Endothelin-A Receptor-Selective Antagonists. *J. Med. Chem.* **1995**, *38*, 1259–1263.
- (52) Patt, W. C.; Edmunds, J. J.; Repine, J. P.; Berryman, K. A.; Reisdorph, B. R.; et al. Structure–Activity Relationship in a Series of Orally Active  $\gamma$ -Hydroxy Butenolide Endothelin Antagonists. *J. Med. Chem.* **1997**, *40*, 1063–1074.
- (53) Nishikibe, M.; Ohta, H.; Okada, M.; Ishikawa, K.; Hayama, T.; et al. Pharmacological Properties of J-104132 (L-753,037), a Potent, Orally Active, Mixed ETA/ETB Endothelin Receptor Antagonist. *Am. Soc. Pharm. Exp. Ther.* **1999**, *283*, 1262–1270.
- (54) Mederski, W. W.; Osswald, M.; Dorsch, D.; Christadler, M.; Schmitges, C.; et al. Benzofuro[3,2-b]pyridines as Mixed ETA/ETB and Selective ETB Endothelin Receptor Antagonists. *Bioorg. Med. Chem. Lett.* **1999**, *9*, 619–622.
- (55) Kukkola, P. J.; Bilci, N. A.; Ikler, T.; Savage, P.; Shetty, S. S.; et al. Isoindolines: A New Series of Potent and Selective Endothelin-A Receptor Antagonists. *Bioorg. Med. Chem. Lett.* **2001**, *11*, 1737–1740.
- (56) Tasker, A. S.; Sorensen, B. K.; Jae, H.; Winn, M.; von Geldern, T. W.; et al. Potent and Selective Non-Benzodioxole-Containing Endothelin-A Receptor Antagonists. *J. Med. Chem.* **1997**, *40*, 322–330.
- (57) *Derwent World Drug Index*; Derwent Information Ltd.: London, 1996 (provided in Catalyst data format by Accelrys, Inc., 9685 Scranton Road, San Diego, CA 92121).
- (58) Lipinski, C. A.; Lombardo, F.; Dominy, B. W.; Feeney, P. J. Experimental and Computational Approaches To Estimate Solubility and Permeability in Drug Discovery and Development Settings. *Adv. Drug. Dev. Rev.* **1997**, *23*, 3–25.
- (59) Balakin, K. V.; Tkachenko, S. E.; Lang, S. A. O. I.; Ivashchenko, A. A.; Savchuk, N. P. Property-Based Design of GPCR-Targeted Library. *J. Chem. Inf. Comput. Sci.* **2002**, *42*, 1332–1342.
- (60) *Ensemble. A New Database Affording a Unique, Integrated View of Drug Information*; Prous Science: Barcelona, Spain, 2001; <http://www.prous.com>.
- (61) Maybridge Chemical Company. *The Maybridge Database*; Daylight Chemical Information Systems, Inc.: Mission Viejo, CA, 2001 (provided in Catalyst data format by Accelrys, Inc., 9685 Scranton Road, San Diego, CA 92121).
- (62) Webb, M. L.; Patel, P. S.; Rose, P. M.; Liu, E. C. K.; Stein, P. D.; et al. Mutational Analysis of the Endothelin Type A Receptor (ETA): Interactions and Model of the Selective ETA Antagonist BMS-182874 with the Putative ETA Receptor Binding Cavity. *Biochemistry* **1996**, *35*, 2548–2556.
- (63) Cramer, R. D., III; Patterson, D. E.; Bunce, J. D. Comparative molecular field analysis (CoMFA). 1. Effect of shape on binding of steroids to carrier proteins. *J. Am. Chem. Soc.* **1988**, *110*, 5959–5967.
- (64) Tafi, A.; Costi, R.; Botta, M.; Di Santo, R.; Corelli, F.; et al. Antifungal Agents. 10. New Derivatives of 1-[(Aryl)[4-aryl-1H-pyrrol-3-yl]methyl]-1H-imidazole, Synthesis, Anti-Candida Activity, and Quantitative Structure–Analysis Relationship Studies. *J. Med. Chem.* **2002**, *45*, 2720–2732.
- (65) Patt, W. C.; Cheng, X. M.; Repine, J. T.; Lee, C.; Reisdorph, B. R.; et al. Butenolide Endothelin Antagonists with Improved Aqueous Solubility. *J. Med. Chem.* **1999**, *42*, 2162–2168.
- (66) Liu, G.; Henry, K. J.; Szczepankiewicz, B. G.; Winn, M.; Kozmina, N. S.; et al. Pyrrolidine-3-carboxylic Acids as Endothelin Antagonists. 3. Discovery of a Potent, 2-Nonaryl, Highly Selective ET<sub>A</sub> Antagonist (A-216546). *J. Med. Chem.* **1998**, *41*, 3261–3275.

JM031041J